APPLICATION OF NONLINEAR GENERALIZED MINIMUM VARIANCE TO THE NADIR PROBLEM IN 2-AXIS GIMBAL POINTING & STABILIZATION

Petros Savvidis*[a], David Anderson[b], Mike Grimble[c]

[a,b]University of Glasgow/Aerospace Dept., James Watt South Buil., University Av., Glasgow, UK

[c]University of Strathclyde/Industrial Control Centre, Graham Hills Buil., George St., Glasgow, UK.

ABSTRACT

Precision tracking applications using two-axis gimbal or antenna actuation systems suffer from a singularity when the inner axis reaches +-90 degrees. This is known by various terms - the keyhole singularity, gimbal lock or the nadir problem. Practically, sightline control is degraded and often lost in a neighborhood of this singularity. In this paper, two nonlinear control algorithms are applied to sightline pointing and stabilization control in the neighborhood of the nadir; the traditional cosecant correction and the nonlinear generalized minimum variance technique. Both controllers were tested against a validated model of an Aeromech TigerEye turret.

Keywords: gimbals, sightline, tracking, stabilization, optimization, control, NGMV, nonlinear, minimum variance

1. INTRODUCTION

Asymmetric warfare – a large conventional army against much smaller terrorist or 'insurgent' groups – has been the defining characteristic of recent military conflicts involving UK and US armed forces. Without clear battlefield lines the identification of and defence against hostile threats has seen a rapid increase in the demand for effective and reliable airborne electro-optic (EO) systems. EO systems fall into two broad classes: Intelligence, Surveillance and Reconnaissance (ISR) systems and Defensive Aid Suite (DAS) systems. Both use similar optical systems technology, but the very real operational differences demand substantially different solutions. For example, an ISR system must have long-range imaging capability, which in turn requires high-resolution imagers and extremely precise sightline stabilization systems to minimize jitter. A DAS system however needs an incredibly agile sightline to ensure that incoming threats to the host platform are properly tracked and interrogated/defeated. This is especially true for Directed Infra-Red Countermeasures (DIRCM) systems.

Two crucial features of EO countermeasures devices carried by airborne vehicles may benefit from the application of modern control: tracking of agile moving targets and own-ship motion sightline stabilization. During engagement, when the host platform is attacked by a surface-to-air missile, a fast and precise sightline loop is essential to intercept the missile system via jamming of the missile seeker. Moreover, it is imperative for the tracking system to be able to operate over a full hyper-hemispherical field-of-regard (FoR), as any tracking deficiencies are sure to be exploited by future missile guidance systems and tactics[1]. Sufficient FoR is ensured by a 2-axis gimbal device with one gimbal rotating over the azimuth axis and the other over the elevation. A significant problem exist with this configuration however when the target moves such that the line-of-sight (LoS) vector approaches the azimuth axis, at around -90 degrees in elevation, the system loses one degree of freedom and is therefore unable to maintain accurate track. Often this degree-of-freedom loss is known as one of the following interchangeable terms – "gimbal lock", "keyhole singularity" or "Nadir cone", although we shall use the latter for the remainder of this paper. Practically, the engagement kinematics driving tracking in the neighbourhood of the nadir require significant agility from the outer, azimuth gimbal axis, to the limit that LoS vector tracking through the singularity when the LoS and azimuth axis are collinear results in infinite acceleration & rate demands to the OG axis. Obviously, the acceleration demands within this range are high enough to saturate the servos, leading to large tracking errors that heavily impair the precision of the system[2].

*psavvidi@eng.gla.ac.uk

Automatic Target Recognition XX; Acquisition, Tracking, Pointing, and Laser Systems Technologies XXIV; Optical Pattern Recognition XXI, edited by F. A. Sadjadi, A. Mahalanobis, S. L. Chodos, W. E. Thompson, D. P. Casasent, T.-H. Chao, Proc. of SPIE Vol. 7696, 76961I · © 2010 SPIE · CCC code: 0277-786X/10/$18 · doi: 10.1117/12.849523

Various techniques have been used in the past to overcome the Nadir problem. The simplest is the orientation of the axes of the turret such that the nadir singularity lies outside the operational region of the system. However, this approach is unsuitable for a DIRCM system due to the need for hyper-hemispherical coverage. The second method, also an opto-mechanical solution, is to add additional axes to the pointing and stabilisation system. Unfortunately this approach increases the size, complexity and initial unit price in addition to comparatively reducing mean-time-between-failure and hence raising operational costs. Transition from military to civilian protection DIRCM systems using multi-axis technology is therefore not practical. The third approach is to reduce the size of the nadir cone by using a faster actuation mechanism, requiring high-performance motors/sensors etc. with the inevitable financial penalties. The fourth approach and the one investigated in this paper is the use of non-conventional sightline controllers to mitigate the effect of nadir singularity on tracking error.

As will be shown later in this paper, operation in the neighbourhood of the nadir presents at least two significant nonlinearities to the sightline control engineer. The first is the singularity introduced earlier. The second is a kinematic nonlinearity due to the difference between the cross-elevation axis (as measured in the imager frame) and the outer gimbal (azimuth) axis. Having two significant nonlinearities in the feedback loop would naturally suggest that a nonlinear control design technique should be applied to the problem. Luckily, a number of nonlinear control laws have been proposed in recent years, including sliding mode control, adaptive backstepping, LMI optimization, nonlinear H-infinity control, feedback linearization and direct Lyapunov methods[3-8]. However, most of the nonlinear controller design techniques mentioned are difficult to use, steeped in complex mathematics and often counter-intuitive tuning. The Nonlinear Generalised Minimum Variance (NGMV) technique developed by Grimble et.al.[9] provides a framework that attempts to isolate the nonlinearities in the system from the sightline control designer. Once the nonlinearities in the system captured in the modelling process are included into the NGMV synthesis, controller tuning is achieved via simple weight selection. The NGMV was designed specifically to yield a nonlinear controller which can be easily designed and commissioned. Therefore, it is an ideal candidate technique for sightline control of a two-axis system.

The structure of the paper is as follows. In section 2 an overview of the Glasgow University sightline control laboratory is presented. This is followed in section 3 by derivation and validation of mathematical models of the turret and external tracking loop that form the heart of the lab. In section 4 an overview of the theory underpinning the NGMV technique is presented and this is followed in section 5 by some simulation results comparing linear, standard nonlinear and NGMV controllers in the neighbourhood of the nadir. Conclusions and recommendations for future work are given in section 6.

2. SIGHTLINE LAB

The Sightline Control Laboratory (SCL) of the University of Glasgow is a bespoke research and teaching facility designed to assist applied research in the areas of pointing, stabilization, tracking and image processing of electro-optic systems – known collectively by the term Sightline Control. The remit of the lab is to provide a hardware-in-the-loop functional testing and analysis facility for all aspects of sightline control, irrespective of the particular unit under test.

2.1 Lab Overview

In the configuration used for this research, an Aeromech TigerEye 2-axis visible band electro-optic turret was used, (see Figure 1 below). The turret is mounted on a tripod about 1.50m height and 2.50m distance from the projector screen. In general, the HD projector is used to display high-definition video of interesting operational vignettes designed to push the tracking loop to its performance limits, in both track creation/association and kinematic prediction. In this set of experiments only the track-loop dynamic response is of interest. Consequently, the projected target is a simple white ball against a blue background, programmed to move along either a circular or vertical trajectory. Each trajectory is specified in a world coordinate system which, for the circular trajectory consists of the y and z axis of the ball defined as sinusoidal functions, the parameters of which define the circle radius and revolution time. For the experiments that follow, the target motion frequency was set at 0.1Hz with a projected image sample rate of 100Hz.

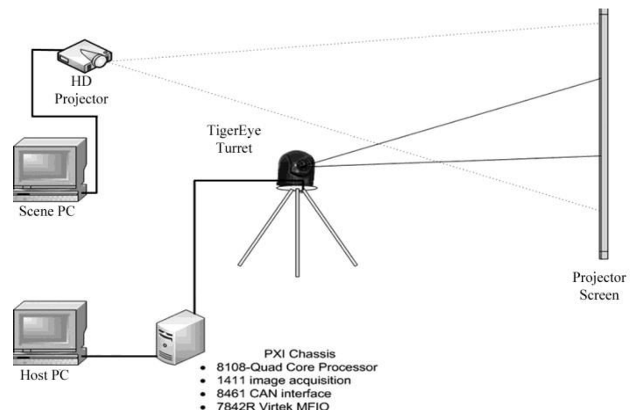

Figure 1, Schematic overview of the sightline control laboratory.

Communication with the TigerEye is performed over a high-speed CAN bus and an RS232 video link. These are interfaced to the host PC using a National Instruments PXI chassis with video framegrabber and CAN bus interface cards. The TigerEye operates in a number of different command modes – position mode, rate mode, stabilized rate mode, body-referenced etc. To implement an external track loop, the TigerEye should be commanded to operate in rate mode, which means that commands sent to the turret over the CAN bus will be interpreted as rate loop demands for each axis. Figure 2 demonstrates a summarizing schematic of the system:

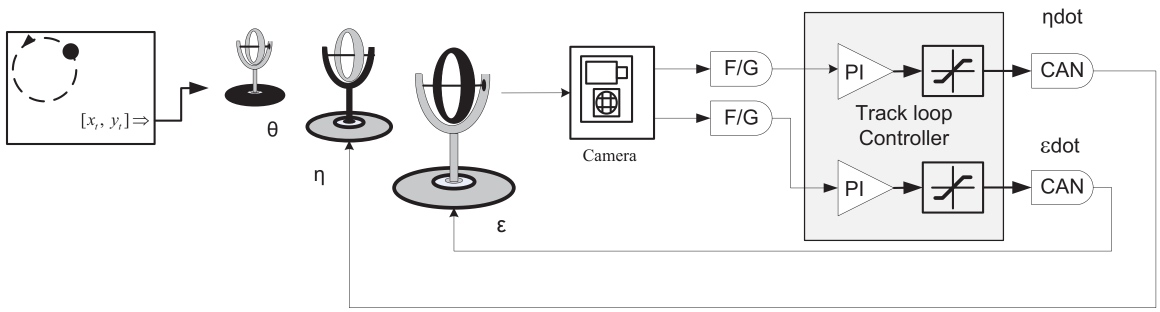

Figure 2, Tracking System Configuration

The measurement for the elevation displacement is taken directly as the vertical pixel displacement, given the camera is fixed to inner gimbal. This measurement then passes through a scaling factor to convert from pixel error to angle error, inside the processing unit where the comparison is taking place, and converted into rate demand. Likewise, the measurement for the azimuth displacement is taken in terms of horizontal pixel displacement, which is a measurement also obtained from the camera fixed onto the inner gimbal. The second error measurement does not represent the actual azimuth error but the azimuth with respect to the inner gimbal defined as the 'cross-elevation'[10]. Using the cross-elevation to control the azimuth axis gimbal can cause problems, as follows.

2.2 Simulation model

2.2.1 Kinematics

The following analysis explains how a change in target position relates to demanded gimbal angles for accurate tracking. Say that the line-of-sight rests on the waterline (zero azimuth and elevation angles) prior to tracking a displacement in the target axes. As shown in Figure 2, there are three principle rotations to consider: base tilt θ, which transforms from world axes to base axes, azimuth (outer gimbal) rotation about the TigerEye z-axis (η) and then an elevation (inner gimbal) rotation about the y-axis, ε. As the camera is carried with the inner gimbal, the image and inner gimbal axes are assumed coincident (neglecting alignment tolerances). Therefore the target position in image axes is given by,

$$x_{los\_im} = (T_\varepsilon T_\eta T_\theta) x_{los_{geo}} \tag{1}$$

Where $T_\varepsilon, T_\eta, T_\theta$ are the direction cosine transformation matrices for the elevation, azimuth and base tilt angles respectively. To recover the off-boresight angle errors needed to drive each track loop controller, the actual target position is projected onto the surface of a unit sphere centered at the image plane. A simple conversion from Cartesian to polar coordinates recovers the actual error angles as measured by the TigerEye imager.

The main problem this research deals with is an implication occurring in the kinematics, when the turret is tracking a target which moves near or past the -90 degrees elevation angle. Then the sightline axis becomes aligned with the outer gimbal rotation axis and the system loses one degree of freedom, Figure 3.

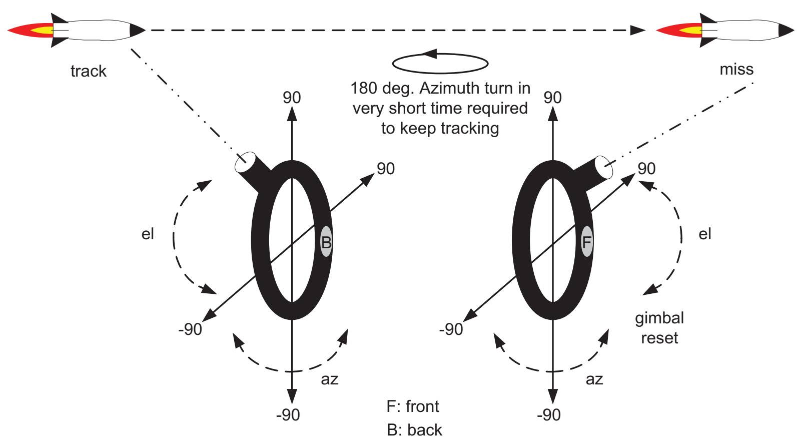

Figure 3 Tracking loss through the Nadir

Operation of the LoS near this condition – inside the nadir cone – introduces two significant problems. The first is the mechanical singularity arising from the loss of a degree of freedom at the nadir, Figure 3. Physically this manifests as the inability of the outer gimbal (azimuth) to perform the necessary instantaneous 180 deg. due to drive/motor saturation and tracking is lost. There is little can be done here without preview or predictive 'shooting' methods[1]. A second nadir nonlinearity arises from the use of cross elevation error as the measurement driving the azimuth motor. In the transformation required to take the cross-elevation back to actual azimuth angle, shown in Equation 2 below, the cross-elevation error δu is multiplied by the cosine of the elevation gimbal angle.

$$\delta\eta_{err} = G_{rad/pix}\begin{bmatrix}\cos(\varepsilon) & 0 & \sin(\varepsilon)\\ 0 & 1 & 0\\ -\sin(\varepsilon) & 0 & \cos(\varepsilon)\end{bmatrix}\begin{bmatrix}0\\0\\\delta u\end{bmatrix} = \begin{bmatrix}0\\0\\\cos(\varepsilon)\delta u\end{bmatrix} \tag{2}$$

As the angle ε increases, there is effectively a reduction in the azimuth track loop gain equivalent to $\cos(\varepsilon)$. At the nadir, the cross-elevation and azimuth axes are orthogonal leading to no effective control in the azimuth track loop. This is the nadir problem this paper will use NGMV to mitigate.

2.2.2 Gimbal Axes Equations

By first principle modeling, the turret system simplicity consists of two servo-motors, one for each gimbal. These rate loops are considered decoupled in this particular application, having no interacting reaction torque effects from one to the other. Consequently the two paths are individually linear and can be easily described by Newton 2nd rotational law of motion as:

$$\begin{gathered}\bar{J}_I\hat{\dot{\omega}}_I(t) + \left(\hat{\omega}_I(t) \times \bar{J}_I\hat{\omega}_I(t)\right) = \hat{L}_I(t) \;\; with \;\; \hat{L}_I(t) = [T_{IC}, T_{Iro}] - [T_{IU}] - [T_{If\omega(t)}]\\ and\\ \bar{J}_O\hat{\dot{\omega}}_O(t) + \left(\hat{\omega}_O(t) \times \bar{J}_O\hat{\omega}_O(t)\right) + \left(\hat{L}_I(t)\right)_O = \hat{L}_O(t) \; with \;\; \hat{L}_O(t) = [T_{OC}, T_{Oro}] - [T_{OU}] - [T_{Of\omega(t)}]\end{gathered} \tag{3}$$

where, J is the inertial matrix and L the sum of the kinematic torques around the equivalent gimbal which, apart from the control torque T_C, include friction and cable restrain torques $T_{f\omega(t)}$, reaction torques T_{ro} acting on the outer gimbal by the inner, and mass imbalance torques T_U about each gimbal[10].

2.3 The Cosecant Correction

One of the methods used to encounter the Nadir tracking consists of directly adjusting the cross-elevation error signal with the use of a secant function to cancel out the cosine in the denominator, Figure 4. Moreover, alternative transformations, like the quaternion, cannot be employed as the problem itself is a result of the turret's physical attributes rather than just an implication of the modeling kinematics.

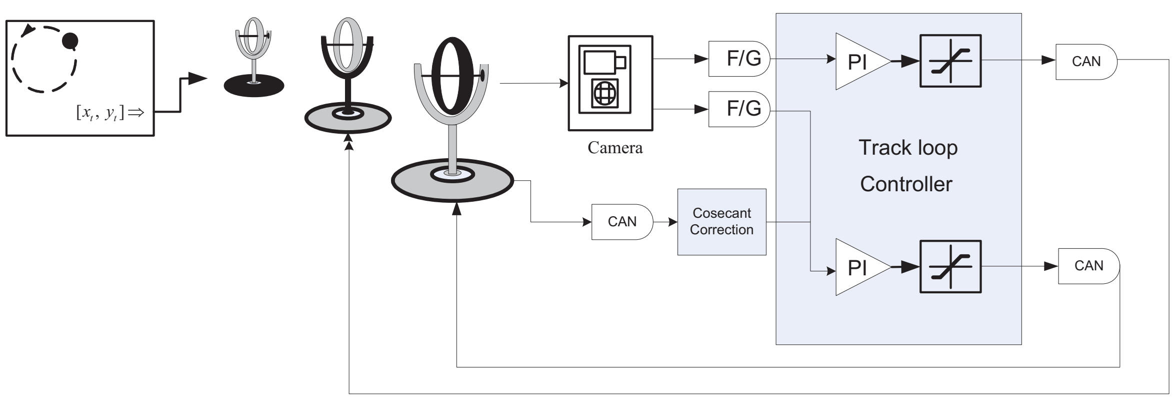

Figure 4 Signal flow for the cosecant correction controller.

To implement the cosecant correction controller, the actual inner gimbal angle is obtained from the telemetry message the TigerEye periodically transmits over the CAN bus. In the results to follow there are some slight synchronization errors between CAN bus reporting and the imager frame rate, but not sufficient to disrupt the action of the controller. Finally, the cosecant correction controller should have a roll-off close to the actual nadir, otherwise infinite gain would be injected into the azimuth axis track loop.

3. MODEL VALIDATION

To test the performance of the NGMV controller, an accurate model of the TigerEye is required prior to creating and commissioning a labview version.

3.1 Model identification

A frequency domain identification strategy was used to extract the transfer functions of each axis. Each transfer function should relate the rate command to the actual gimbal axis rate, as reported by the stabilization loop gyros over the CAN bus. The nominal CAN bus trajectory reporting frequency is 10Hz and the imager frame rate is 30Hz. Logarithmically-spaced input sinusoids of frequencies from 0.05 to 4 Hz excited each axis in turn and, using SCL LabView code, the system frequency response function for each input frequency were computed. This data was converted into gain and phase plots in Matlab, from which accurate transfer functions were obtained. The spectral characteristics for the tilt and pan rate loops are compared against the identified ones in figure 5.a and 5.b respectively.

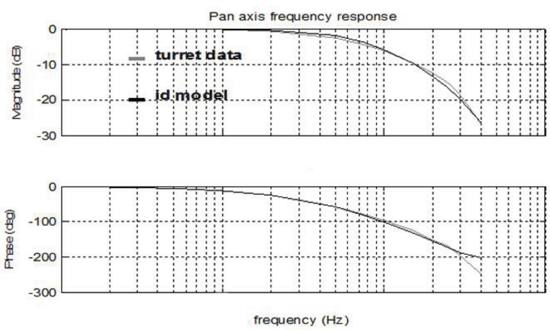

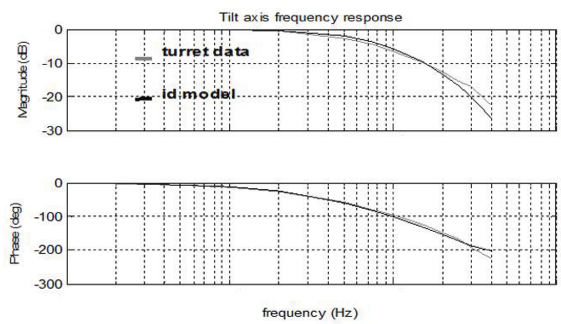

Figure 5, tilt & pan rate loop identification

3.2 Model validation

To use a mathematical model for control design in the neighborhood of the nadir, the accuracy of the model in this region has to be determined. The moving target and full gimbal kinematics of the problem were implemented along with the identified turret model in Matlab. The system was simulated for the case where the turret tracks a ball moving along a circular trajectory in 0.1 Hz and under various base tilt angles from 0 (waterline) to 90 deg. (Nadir). Given the same scenarios, the real turret was tested and the rate commands along with the spectral error compared to those of the simulation, Figure 6. On the pan graph corresponding to -90 degrees base tilt angle the saturation in the azimuth gimbal motor can be seen after which the camera captures the target again but only in the case where the target moves relatively slowly.

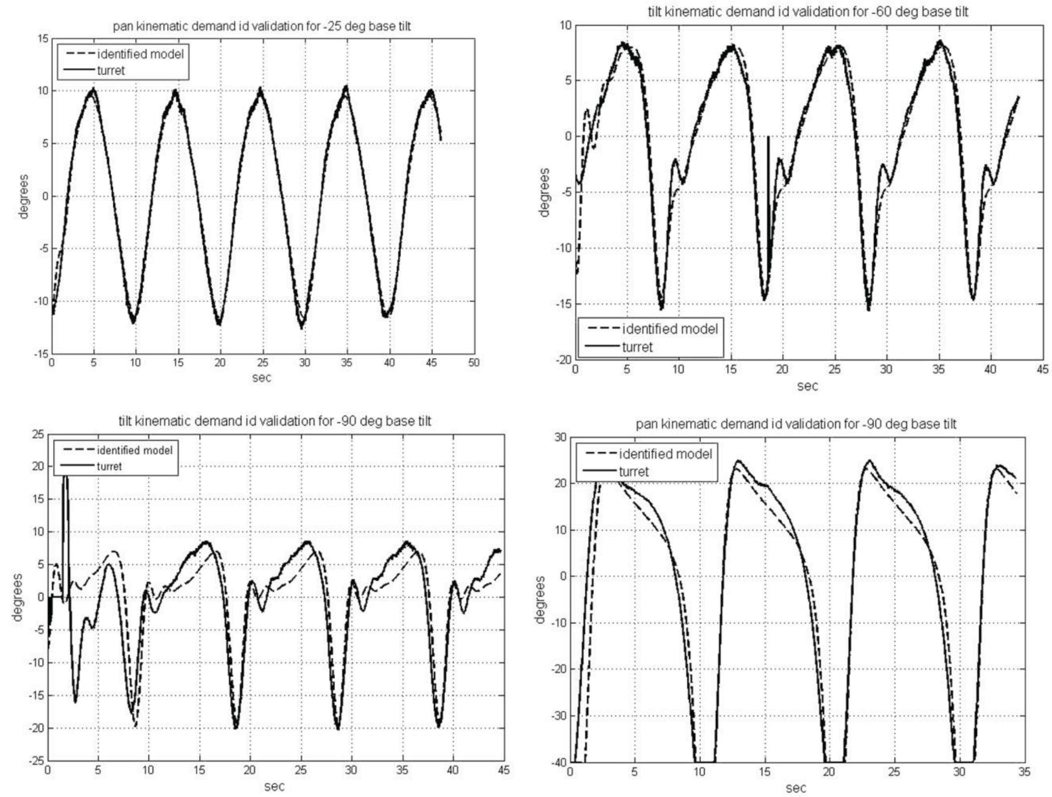

Figure 6 Validation results for various base tilt angles

As we can see from Figure 6, regardless of the mismatch occurring due to phase differences and potential jitter (varying sample rate) on the CAN bus, the identified data holds a model representation accurate enough to stand as the simulation basis.

4. NONLINEAR GENERALIZED MINIMUM VARIANCE CONTROL

Although the individual rate loops are not nonlinear, the total system demonstrates the inverse cosine nonlinearity which appears as a singularity on the reference signal. That makes the situation peculiarly difficult to be dealt with a conventional nonlinear control scheme. In this paper the Nonlinear Minimum Variance Controller is introduced, having a feature that allows various nonlinearities to be explicitly included inside the controller.

4.1 Overview

Based on the development of the Minimum Variance controller[11] and the later work on the Generalized Minimum Variance control, where a control signal costing term has been added[12], Grimble developed the Nonlinear Generalized Minimum Variance Control scheme applied in nonlinear SISO or MIMO stochastic non-minimum phase systems. The NGMV combines features of the Smith Predictor, in dealing with pure delays and process deadbeats, and of the IMC as well, containing an internal model of the process. The uncertainty though, that might occur between the modeled and the actual plant is regulated with the use of two weightings, penalizing the control and the error signal.

Unlike its predecessors the use of dynamic cost-function weightings, allow regulation within a wider operating range without the need for local linearization. The plant description is treated in a very general nonlinear operator form, which may be consisted of state-space models, transfer operators or nonlinear look up tables. The reference and disturbance models are described by linear subsystems with some loss of generality. Input-output nonlinearities appear as black boxes and this gives the algorithm a great advantage as it takes the modeling of the nonlinearity out of concern. Solving the optimal control law only involves the output and the control signal hence the nonlinear subsystem model is needless. Although in the case that it is available it can be directly used in the algorithm[12].

The general model description feature of the algorithm extends to the weightings as well which can be constant, dynamic containing nonlinearities and state-dependent, as it is currently investigated, given that they are open-loop stable. Additionally unlike feedback linearization methods the plant model does not need to be affine.

Stability for linear systems is ensured when the combination of the control and error weightings is strictly minimum phase. In the nonlinear case the plant operator must have a stable inverse. It is shown that if there is a PID controller that will stabilize the nonlinear system, without transport delay elements, then a set of cost weightings can easily be defined to guarantee the existence of this inverse and thus ensure the stability of the closed loop[9]. Figure 7 summarizes a simplified formulation of the NGMV while in Figure 8 the internal structure of the various parts in state-space formulation is demonstrated. In this form the Smith Predictor, IMC and MV features are apparent.

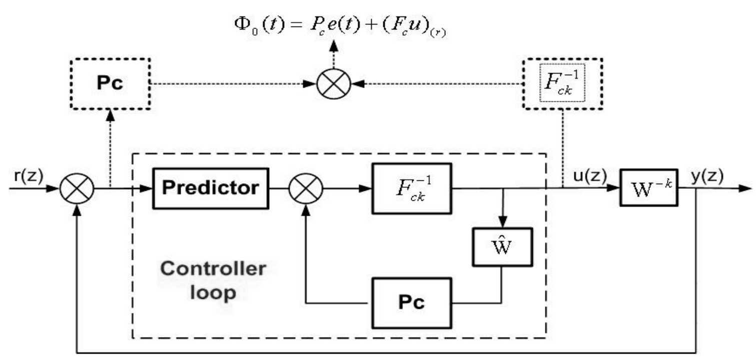

Figure 7 the NGMV control loop formulation

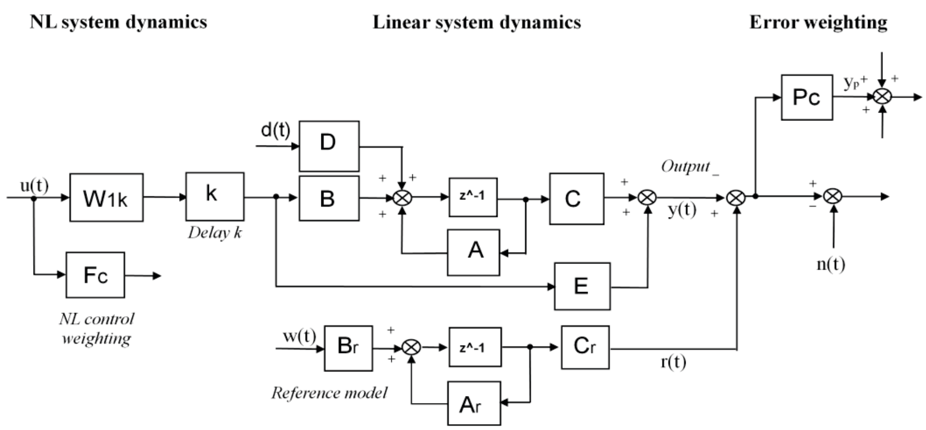

Figure 8 plant, reference and disturbance definition in combination with the NGMV weightings

Total NL Part:

$$(Wu)_{(t)} = (W_{0k}W_1u)_{(t)} = (W_{0k}z^{-k}W_1u)_{(t)} \tag{4}$$

Total NL and Linear State Equations:

$$x_1(t+1) = A_1 x_1(t) + B_1 y_1(t) + D_1 \xi_1(t)$$
$$y(t) = Cx(t) + Eu_1(t-k) \tag{5}$$

with $$x_1(t) = [x_r^T(t)\ \ x_p^T(t)]^T,\ A_1 = \begin{bmatrix} A_r & 0 \\ B_p C_r & A_p \end{bmatrix},\ B_1 = \begin{bmatrix} 0 \\ -B_p \end{bmatrix},\ D_1 = \begin{bmatrix} D_r \\ 0 \end{bmatrix}$$

The output as seen in Figure 8 and using Equation 5 can be written as:

$$x(t+1) = Ax(t) + u_1(t-k) + D\xi(t) \tag{6}$$

and from Equation 6 the future outputs can be derived iteratively:

$$x(t+2) = A^2 x(t) + ABu(t) + Bu_1(t+1-k) + AD\xi(t) + D\xi(t+1) \tag{7}$$

etc. These steps are summed up as:

$$x(t+i) = A^i x(t) + \sum_{j=1}^{i} A^{i-j}\ (Bu_1(t+j-1-k) + D\xi(t+j-1)) \tag{8}$$

and the future k-steps ahead weighted output is:

$$\hat{y}_p(t+i+k/t) = C_p A^i \hat{x}(t+k/t) + \sum_{j=1}^{i} C_p A^{i-j}\ \big(Bu_1(t+j-1) + D\xi(t+j+k-1)\big) + E_p u_1(t+i) \tag{9}$$

4.2 The NGMV control problem

A time-varying Kalman filter is used to retrieve the initial states in Equation 9:

$$\hat{x}(t+1/t) = A\hat{x}(t/t) + Bu_1(t-k) + D\bar{\xi}(t)\ \ \text{(predictor)} \tag{10}$$

$$\hat{x}(t+1/t+1) = \hat{x}(t+1/t) + K_f(t+1)(e_0(t+1) - \hat{e}_0(t+1/t))\ \ \text{(corrector)}$$
$$\hat{e}_0(t+1/t) = C_e\hat{x}(t+1/t) - Eu_1(t+1-k) - \bar{v}(t) \tag{11}$$

NGMV uses the same cost function as the Minimum Variance controller, $J = E\{trace\{\varphi_0(t)\varphi_0^T(t)\}\}$ where $\varphi_0(t) = P_c e(t) + (F_c u)_{(r)}$. Embedding the future output signal in the cost function holds:

$$\hat{\varphi}_0(t+k_0/t) = \hat{y}_c(t+k_0/t) + (F_{ck}u)_{(t)} = C_\varphi(t+k_0)A\hat{x}(t/t) + \Big(\big(C_\varphi T + E_\varphi\big)W_{1k} + F_{ck}\Big)u(t) \tag{12}$$

The cost function can be written in prediction and prediction error terms as:

$$J = E\{\hat{\varphi}_0(t+k_0/t)^T\hat{\varphi}_0(t+k_0/t)\} + E\{\tilde{\varphi}_0(t+k_0/t)^T\tilde{\varphi}_0(t+k_0/t)\} \tag{13}$$

The prediction is independent of the control action hence setting it to zero minimizes the cost function and that gives the NGMV law which is:

$$u(t) = -F_{ck}^{-1}(C_\varphi A\hat{x}(t/t) + (C_\varphi T + E_\varphi)(W_{1k}u)_{(t)}) \tag{14}$$

4.3 Weightings selection

When the control and error weightings are selected to be strictly minimum phase then stability for linear systems is ensured. For nonlinear systems though we assume that the related operator equation must have a stable inverse. Moreover it is shown that if there are PID parameters stabilizing the open-loop process, then these can be used for an NGMV weighting initial selection, with performance similar to that of the PID[9].

5. RESULTS

To quantify the performance of the NGMV controller, the track error returned for scenario 2 – target motion in the *z*-axis only – was computed for a basic PI controller, PI+cosecant correction and NGMV. The tracking performance for a close nadir pass scenario (1cm screen coordinates corresponding to a nadir miss angle of 2.3deg), is shown below in figure 9. This close to the nadir singularity the azimuth demand resulting from the kinematics changes rapidly with a large error forming immediately prior to the nadir due to the rate limit on the azimuth gimbal. In all three responses, the underlying PI controller is identical, differences in the responses due solely to the additional nonlinearities in the cosecant correction and NGMV controllers.

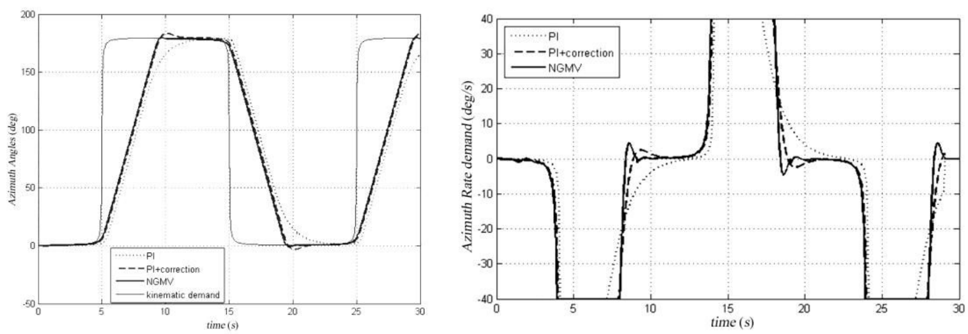

Figure 9 Kinematic and achieved azimuth angles for a 1cm nadir pass scenario.

All three controllers are very well damped with minimal overshoot and little or no ringing. The response of the PI controller is the slowest of the three, as expected due to the presence of the cos(ε) gain term in the measurement path (note: although the gain has reduced, the large error signal forces saturation of the rate loop). Relating this result to the key requirements of a DIRCM tracker (maximise energy on target), the NGMV controller settles down after the first nadir pass at 10seconds, the PI+Cosecant settles after 11sec and the PI 12sec. This suggests the NGMV controller would provide more time-on-target of the DIRCM defeat laser, increasing the probability of missile confusion.

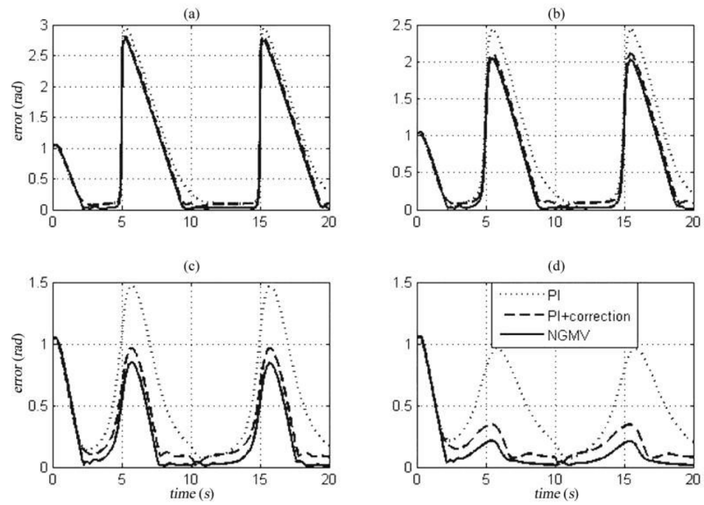

Figure 10 Total LoS track error for nadir pass geometries of (a) 1cm, (b) 5cm, (c) 20cm and (d) 40cm.

While tracking performance close to the nadir is important, controller performance should be maintained throughout the field-of-regard. Figure 10 shows the radial track error (angle between boresight and target vectors) for four nadir pass conditions: 1cm, 5cm, 20cm and 40cm. In all cases the same trend is observed – cosecant correction outperforms the PI alone and the NGMV consistently provides better tracking performance.

6. CONCLUSIONS

A number of contributions to the sightline control literature were presented and discussed in this paper. First, the architecture, functionality and intended operation of the Sightline Control laboratory were presented. The suitability of the SCL hardware for investigation of track loop operation in the neighborhood of the nadir was demonstrated and the process of system modeling, identification and validation discussed. The mathematical models of both gimbal axes and SCL kinematics were validated against experimental results.

Through a detailed derivation and explanation of the key design parameters in NGMV controller design, the suitability of an NGMV track-loop controller in operation close to the nadir was shown. The primary benefit of this technique is the ability to include the system nonlinearities, the azimuth axis measurement singularity in this case, directly within the controller but shielded from the designer. The NGMV controller was consistently the best performing controller with minimal additional tuning. This suggests NGMV is a practical synthesis technique for sightline controllers.

REFERENCES

[1] Anderson, D., Loo, M. and Brignall N., "*Fast Model Predictive Control of the Nadir Singularity in Electro-Optic Systems*", Journal of Guidance Control & Dynamics, 32(2), 626-632, (2009) .

[2] Rue, A. K., "*Stabilisation of precision electro-optical pointing and tracking systems*", IEEE Transactions of Aerospace Electronic Systems, Vol. AES-5, No.5, 1969, pp. 805-819.

[3] Utkin, V., Guldner, J. and Shi, J., "*Sliding Mode Control in electromechanical systems*", Taylor & Francis Inc., 1999.

[4] Léchevin, N. and Rabbath, C.A., "*Backstepping Guidance for Missiles Modeled as Uncertain Time-Varying First-Order Systems*", Proceedings of the 2007 American Control Conference, New York, USA 2007.

[5] Henrion, D., Arzelier, D. and Peaucelle., D., "*Positive Polynomial Matrices and Improved LMI Robustness Conditions*", Automatica, Vol. 39, No. 8, pp. 1479-1485, August 2003.

[6] Morari, M. and Zafirou, E., "*Robust Process Control*". Prentice-Hall International, 1989.

[7] Corriou, J., "*Process Control: theory and applications*", Springer-Verlag, 2004.

[8] White, W., Patenaude, J., Foss, M. and Garcia, D., "*Direct Lyapunov approach for tracking control of underactuated mechanical systems*", Proceedings of the 2009 conference on American Control Conference, Missouri, USA 2009.

[9] Grimble, M., "*Nonlinear Generalized Minimum Variance Feedback, Feedforward and Tracking Control*", Automatica 41 p. 957-969 2005.

[10] Kennedy, P. J. and Kennedy, R. L., "*Direct Versus Indirect Line of Sight (LOS) Stabilization*", IEEE transactions on control systems technology, vol. 11, no. 1, January 2003.

[11] Astrom, K., "*Introduction to stochastic control theory*", London Academic Press 1979.

[12] Grimble, M., "Design *of Generalized Minimum Variance Controllers for Nonlinear Multivariable Systems*", International Journal of Control, Automation and Systems, October 2005.